БЪЛГАРСКА АКАДЕМИЯ НА НАУКИТЕ • BULGARIAN ACADEMY OF SCIENCES

ПРОБЛЕМИ НА ТЕХНИЧЕСКАТА КИБЕРНЕТИКА И РОБОТИКАТА, **61**
PROBLEMS OF ENGINEERING CYBERNETICS AND ROBOTICS, **61**

София • 2009 • Sofia

A Dynamic Converter of Monophase into Triphase Voltage. Part II: Starting and Control[1]

Zdravko Nikolov, Chavdar Korsemov, Hristo Toshev

Institute of Information Technologies, 1113 Sofia
E-mails: znikolov@iit.bas.bg chkorsemov@iinf.bas.bg toshev@iinf.bas.bg

1. Introduction

The present paper is continuation of Part I (in the same issue) and it investigates the start and control of dynamic converters of monophase into triphase voltage using a standard triphase asynchronous motor with a cage rotor, constructed according to the scheme, shown in Fig. 1, Part I.

2. Converter starting

The dynamic phase converter uses an asynchronous motor with a cage rotor. This type of motors, in spite of its advantages, has got one considerable shortcoming and it is that the start moment is too small. This refers particularly to motors with deep or double jacks. The problem of the starting mode becomes very serious when switching on is made under loading. One of the approaches to improvement of the start characteristics is the monophase swithcing on until nominal revolutions are achieved and after that the motor is switched to symmetric triphase supply.

Steinmets scheme, shown on Fig. 2 is used for monophase supply of a triphase motor. The connected capacitor C diminishes the great asymmetry of the power supply. In order to analyze a non-symmetric triphase network, it is appropriate to

[1]This work is connected with the project "Scientific Support of the Development of a Device, Controlling a Monophase into Triphase Converter", No 210192, realized with the Agency of Small and Medium Sized Enterprises at Ministry of Economy, Energy and Tourism, Bulgaria.

present it as superposition of three networks – symmetric direct, symmetric inverse and a network of null order with the corresonding phases, set to the base selected.

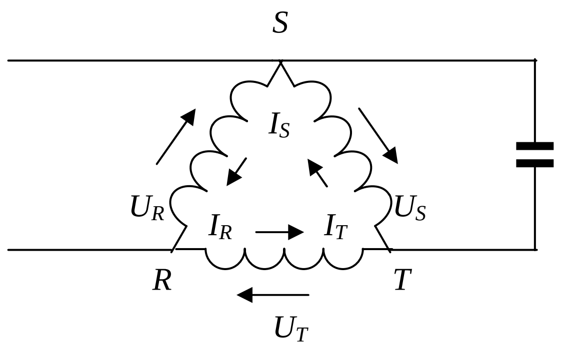

Fig. 2

The first two differ by level and phase and most significant – their phases increase in time in opposite directions and hence they produce rotating moments with opposite signs, if supplying triphase motors. The degree of asymmetry is expressed by the complex coefficient $\dot{k}_u = \frac{\dot{u}_2}{\dot{u}_1}$, which caries information about the relation of the amplitudes and phases. For linear loads similar expansion can be done for the currents $\dot{k}_i = \frac{\dot{I}_2}{\dot{I}_1}$ as well.

The components of null order do not create rotating moments, but can lead to the appearance of current components, and thus to additional losses. When connecting a triangle or isolated null, the voltage components of zero order do not cause currents formation.

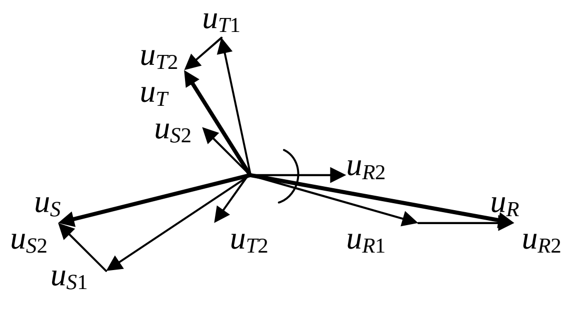

Fig. 3

Fig. 3 shows the vector diagram of the expanded to positive and negative non-symmetric triphase system

$$\dot{u}_2 = \dot{k}\dot{u}_1 .$$

The order of the phases on the vector diagram for positive and negative series is opposite.

The resultant vector diagram obtained shows big asymmetry of the actual network.

The non-symmetric triphase network is unambiguously determined by $\dot{U}_1, \dot{k}_u, \dot{k}_i$ and $\dot{I}_1, \dot{U}_0$.

The decomposition of the actual system into composing – positive, negative and null components, is done according to the relations

$$\dot{u}_1 = \dot{u}_R + a\dot{u}_T + a^2\dot{u}_S,$$

$$\dot{u}_2 = \dot{u}_R + a^2\dot{u}_T + a\dot{u}_S,$$

$$\dots$$

$$\dot{v}_0 = \dot{u}_R + \dot{u}_S + \dot{u}_T.$$

In the expressions $a = e^{J\frac{2}{3}\pi}$ denotes rotation at 120°.

Only triangle connections are considered here, because of the great advantages of the phase converters, which do not contain null components.

Positive and negative components for the impedances may be introduced in a similar way

$$\dot{Z}_1 = \frac{\dot{u}_1}{\dot{I}_1}, \quad \dot{Z}_2 = \frac{\dot{u}_2}{\dot{I}_2}.$$

It is appropriate to present with their help the currents dependence on the slip *S*,

$$\dot{Z}_i(S) = \frac{\dot{u}_i}{\dot{I}_i}.$$

Using the decomposition into symmetric components, Steinmetz connection can be represented by the relations

$$\dot{I}_R = \frac{\dot{u}_1}{\dot{Z}_1(S)} + \frac{\dot{u}_2}{\dot{Z}_2(S)},$$

$$\dot{I}_T = a^2\frac{\dot{u}_1}{\dot{Z}_1(S)} + a^2\frac{\dot{u}_2}{\dot{Z}_2(S)},$$

$$\dot{I}_S = a\frac{\dot{u}_1}{\dot{Z}_1(S)} + a^2\frac{\dot{u}_2}{\dot{Z}_2(S)},$$

$$\dot{u}_S = \frac{1}{j\varpi_0 C}\left(\dot{I}_T - \dot{I}_S\right).$$

From the above relations after some not complex transformations, the following is determined:

$$\dot{u}_2 = \frac{\dfrac{a^2 - a}{j\varpi_0 C\dot{Z}_1(S)} - a}{\left(a^2 - a\right)\left[\dfrac{1}{j\varpi_0 C}\left(\dfrac{1}{\dot{Z}_1(S)} + \dfrac{1}{\dot{Z}_2(S)}\right) + 1\right]}\dot{u}_T.$$

Introducing an additional multiplier $\dot{k}_2$,

$$\dot{k}_2 = \frac{\dfrac{1}{j\varpi_0 C\dot{Z}_1(S)} - e^{-j\frac{5}{6}\pi}}{1 + \dfrac{1}{j\varpi_0 C}\left(\dfrac{1}{\dot{Z}_1(S)} + \dfrac{1}{\dot{Z}_2(S)}\right)}$$

for the positive and negative components it is obtained

$$\dot{u}_1 = (1 - \dot{k}_2)\dot{u}_T,$$

$$\dot{u}_2 = \dot{k}_2\dot{u}_T,$$

and for the coefficients of voltage and current non-symmetry (debalance)

$$\dot{k}_u = \frac{\dot{k}_2}{1 - \dot{k}_2},$$

$$\dot{k}_i = \frac{\dot{Z}_1(S)}{\dot{Z}_2(S)}\dot{k}_v.$$

The symmetry of the voltages on the rotor, after Steinmitz scheme, at monophase supply is obtained at $k_2 = 0$:

$$\varpi_0 C e^{j\frac{\pi}{2}}\dot{Z}_1(S) = e^{j\frac{5}{6}\pi},$$

$$X_C = \frac{1}{\varpi_0 C} = \dot{Z}_1(S)e^{-j\frac{\pi}{3}}.$$

In order to achieve complete symmetry, in this expression the impedance of the motor phase winding must have inductive character with a phase angle $\arg \dot{Z}_1(S) = \dfrac{\pi}{3}$.

In a real asynchronous motor with a cage rotor during the interval immobile rotor – synchronous revolutions, the impedance $\dot{Z}_1(S)$ is altered from almost purely active up to almost purely inductive. During the start the symmetry is obtained in a small area of slippage. At the point of complete balance, in which the motor moment equalizes with that of fully symmetric triphase supply, the module of the impedance determines the value of the necessary capacity $\dfrac{1}{\varpi_0 C} = \left|\dot{Z}_1\right|$.

In [1] a study of the monophase supply of a triphase motor after Steinmetz scheme is discussed. The experimental results from such investigations, given in Fig. 4, show its high efficiency. The motor moment is marked along the ordinate axis for symmetric triphase supply, for monophase with included compensating capacitor, for purely monophase and the resistance moment $\dot{T}_L$ (load) of the motor regarded as a function of the slippage *S*. The start moments (up to achieving nominal revolutions) for triphase supply and for monophase with compensation are close, at that for revolutions above point B the supply compensated develops a higher moment. At point B the impedance $\dot{Z}_1$ equalizes in module with that of the capacitor and phase $\arg \dot{Z}_1 = \frac{\pi}{3}$, which leads to complete triphase symmetry in the supply.

For purely monophase supply the motor moment is considerably smaller, in idle state it is zero, since the positive and negative components u_1 and u_2 are with equal amplitudes and cause motor moments in opposite directions. Driven in any direction, the motor gains resultant motor moment, but it is much smaller than the achieved with other supplies.

The performance of a triphase motor, monophase supplied by a compensating capacitor, especially selected to maximize the start moment, is studied in [2]. After approaching the nominal revolutions, the motor is switched to symmetric triphase supply. It is shown that at such switching on the motor moment raises considerably, which enables turning on under load, and also the rapid achievement of nominal revolutions. The experimental results, described in this paper, show considerable rising of the start moment and multiple shortening of the interval for reaching nominal rotational speed.

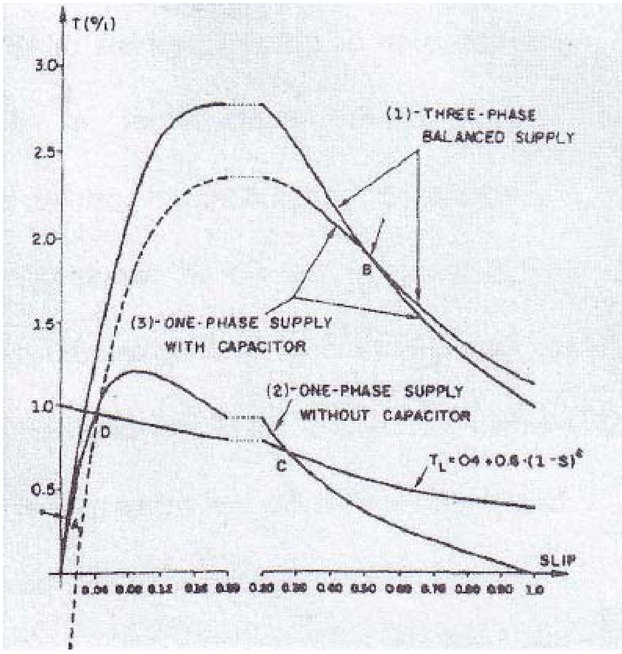

Fig. 4

Fig. 5 shows the relations of the rotational speed and the motor moment in the transient interval for one and the same motor, triphase supplied (Fig. 4) and monophase with a capacitor according to the approach described, from a network of 60 Hz.

The advantages of the second connection are clearly observed. The oscillations of the motor moment are weakly expressed and the nominal revolutions are gained more rapidly. However, a cyclic component of the revolutions with a frequency of 10-12 Hz appears. This component disappears after switching to triphase supply.

3. Converter control

The most common control of the converter is with respect to maximization of the symmetry degree, and a criterion of this may be the maximum of the positive components or the minimum of the negative ones in the decomposition into symmetric components. The control related to maximum is more sensitive, the direction of the impact may be carried by the phase of the negative component. In some special cases the control may be executed not only with respect to the module, but also to the negative component phase.

Herein a triphase converter is considered in triangle connection, the control is attached to the potential of the phase, towards which the compensating capacitors are connected. Such an approach simplifies the control, but the experience shows that it can function quite efficiently, without any complex protection and filter circuits, not influenced by disturbances. In the scheme shown on Fig. 6 the control is attached to clamp L_3.

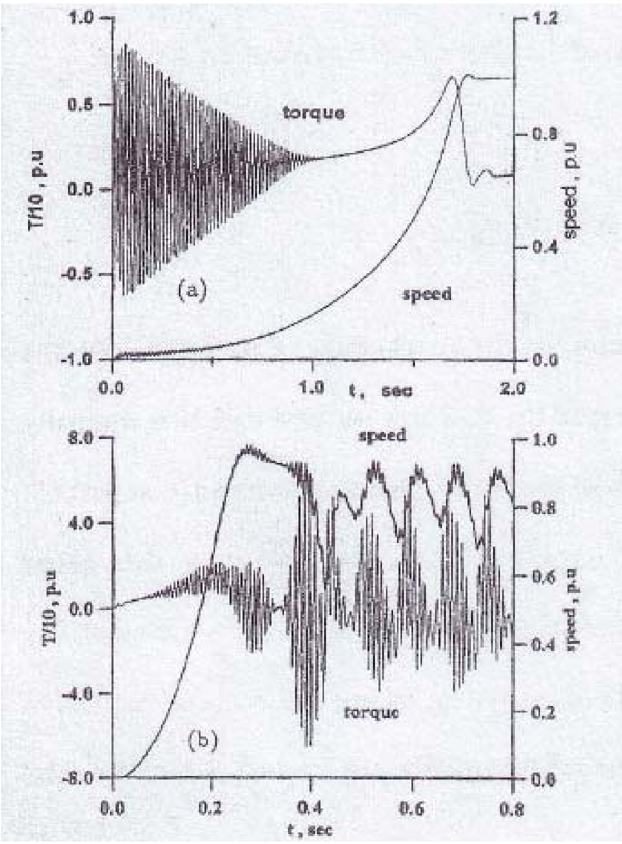

Fig. 5

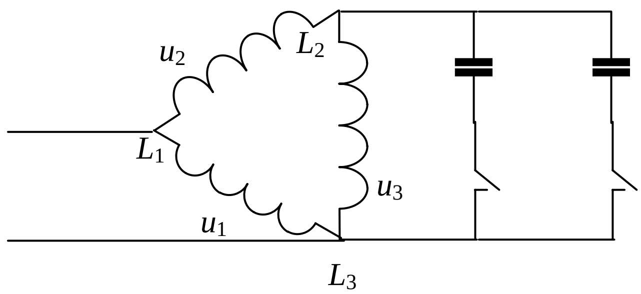

Fig. 6

The triangle connection excludes the appearance of zero components in the decomposition.

The control only with respect to the negative components and their approximation is discussed here. They are defined according to the relation $e_2 = u_1 + a^2 u_3 + a u_2$, where $a = e^{j\frac{2}{3}\pi}$ is a rotating multiplier. Despite of the control accomplishment – digital or analog, due to the large difference in the levels of the primary signals in comparison with the ones in the processing node, it is appropriate to make the necessary rotations in an analog way or with the help of integrating, not differentiating circuits for better noise resistance. This implies the realization of the rotation not in the positive, but in the negative direction.

With a selected common point L_3, the circuit has not direct access to voltage u_2. It is determined by the relation $u_1 + u_3 + u_2 = 0$. The voltage $-u_3$, not u_3 enters the same point.

Taking in mind these considerations, different realizations are possible for determination of the negative components. Herein the basic one, attached to the basic voltage u_1 is defined. Two similar schemes are shown on Fig. 7.

These circuits realize the necessary operations, but they have significant shortcomings as well. They use rotation after a summing operation. One of the rotations is executed with overtaking, using a differentiating circuit. It is advisable all the rotations to be done before signals entry into the control node. Since some of the rotations are sometimes bigger than $\frac{\pi}{2}$, the circuit, realizing them, will be of second order. Due to the large difference between the input and output levels, the realization of such circuits without any intermediate unbinding does not cause any problems. Such a scheme, satisfying these additional requirements, is shown on Fig. 8.

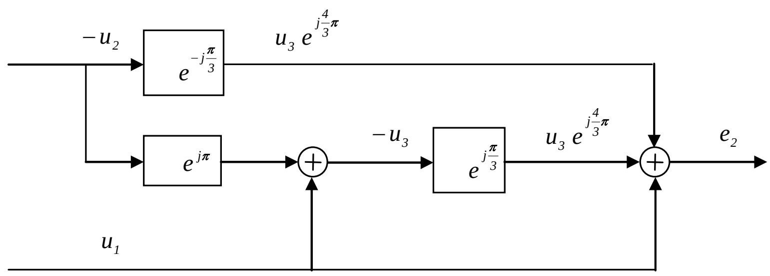

a)

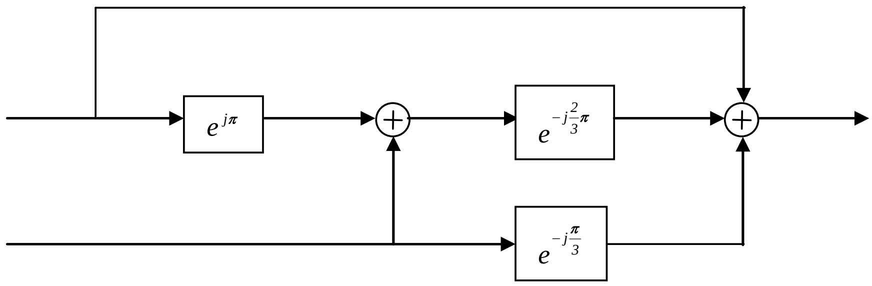

$$u_3 e^{j2\pi} e^{-j\frac{2}{3}\pi} = u_3 e^{\frac{4}{3}\pi} = a^2 u_3$$

b)

Fig. 7

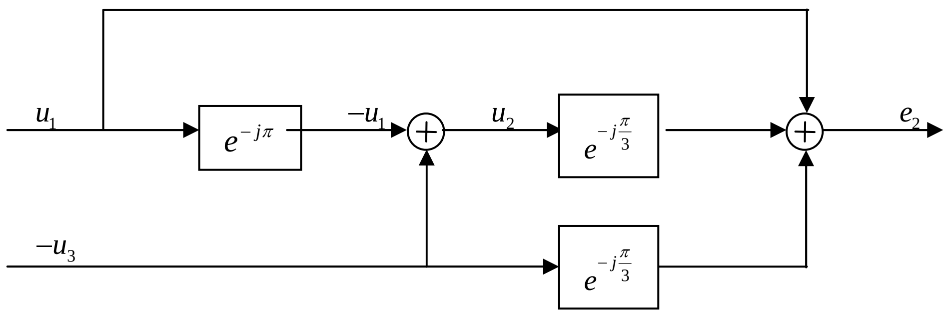

$$u_2 e^{j2\pi} e^{-j\frac{2}{3}\pi} = u_2 e^{\frac{4}{3}\pi} = a^2 u_2$$

Fig. 8

For analog realization of the rotation, the circuits shown on Fig. 9 can be used, for rotations at $\frac{\pi}{3}$ and at $\frac{2}{3}\pi$ respectively.

The transfer coefficient for the first scheme is

$$K = \frac{u_1}{u_0} = \frac{R_2}{R_1} \frac{1}{1 + \frac{R_2}{R_1} + j\varpi R_2 C},$$

$$K = \frac{R_2}{R_1} \frac{1}{\sqrt{\left(1 + \frac{R_2}{R_1}\right)^2 + \left(\varpi R_2 C\right)^2}} e^{-j\varphi},$$

$$\varphi = \operatorname{arctg} \frac{\varpi R_2 C}{1 + \frac{R_2}{R_1}}.$$

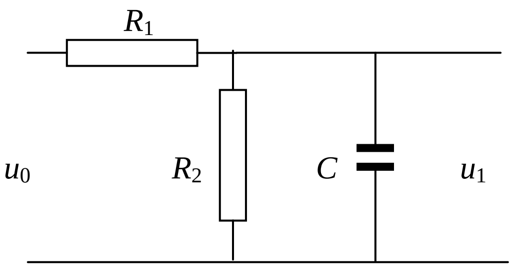

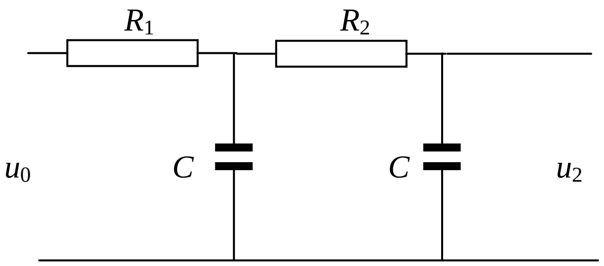

Fig. 9

For rotation at $\frac{\pi}{3}$, it is necessary to have $\varphi = \frac{\pi}{3}$,

$$\operatorname{tg} \frac{\pi}{3} = \sqrt{3} = \frac{\varpi R_2 C}{1 + \frac{R_2}{R_1}},$$

and for the separate values after not complex transformations the following is obtained:

$$|K| = \frac{R_2}{2\left(R_1 + R_2\right)},$$

$$R_1 = \frac{\sqrt{3}}{2|K|\varpi C},$$

$$R_2 = \frac{2|K|}{12|K|} R_1.$$

For $|K| = 10^{-2}$, $C = 1\ \mu\text{F}$, $\varphi = \dfrac{\pi}{3}$, $R_1 = 275.8\ \text{k}\Omega$, $R_2 = 5.628\ \text{k}\Omega$.

For the second scheme the transfer coefficient has the form

$$K = \frac{u_2}{u_0} = \frac{1}{\varpi C R_1}\sqrt{\frac{1}{4+\left(\varpi R_2 C\right)^2}}\,\frac{e^{-j\varphi_2}}{A},$$

where

$$A = 1 + \frac{1}{\varpi R_1 C}\sqrt{\frac{1+\left(\varpi R_2 C\right)^2}{4+\left(\varpi R_2 C\right)^2}}\,e^{j(\varphi_1-\varphi_2)},$$

$$\varphi_1 = \operatorname{arctg}\varpi R_2 C,$$

$$\varphi_2 = \operatorname{arctg}\left(-\frac{2}{\varpi R_2 C}\right),$$

$$A = \operatorname{mod} A = \sqrt{\left(1+\frac{R_2}{R_1}\frac{1}{4+\left(\varpi R_2 C\right)^2}\right)^2 + \left(\frac{R_2}{R_1}\frac{1}{4+\varpi^2 R_2^2 C^2}\right)^2\left(1+\frac{2}{\varpi R_2 C}\right)^2},$$

$$\arg A = \operatorname{arctg}\left[-\frac{\dfrac{2}{\varpi R_2 C}+\varpi R_2 C}{1+\dfrac{R_1}{R_2}\left(4+\varpi^2 R_2^2 C^2\right)}\right].$$

For $R_1 >> R$, $\arg A \to 0$ $\operatorname{mod} A \to 1$ and the transfer coefficient is approximated by

$$|K| = \frac{1}{\varpi R_1 C}\sqrt{\frac{1}{4+\left(\varpi R_2 C\right)^2}},$$

$$\arg K = \varphi = \operatorname{arctg}\left(-\frac{2}{\varpi R_2 C}\right).$$

For $\arg A = \dfrac{2}{3}\pi$, $\operatorname{tg}\varphi = -\sqrt{3}$, and

$$\sqrt{3} = \frac{2}{\varpi R_2 C}, \quad \varpi R_2 C = \frac{2}{\sqrt{3}}.$$

Then $|K| = \dfrac{1}{\varpi R_1 C}\dfrac{\sqrt{3}}{4}$.

For $C = 0.47\ \mu\text{F}$, $|K| = 10^{-2}$, $\varpi = 2\pi.50$ and:

$$R_1 = \frac{\sqrt{2}}{4K\varpi C} = 293 \text{ k}\Omega,$$

$$R_2 = \frac{2.10^6}{\sqrt{3}.2\pi.50.0,47} = 7.82 \text{ k}\Omega.$$

The capacitors are selected with larger values for good resistance to disturbing voltages.

The operation related to rotation can be purely digital. A register for every of the voltages is sufficient, in order to support the discretes for one period of the network. The rotation is determined by the output cell of the register, from which the output signal is taken. The number of discretes for a network period is defined by the desired accuracy of determination of the module and the phase of the inverse component e_2.

The phase of the inverse component e_2 can be determined by a phase discriminator, as shown on Fig. 10.

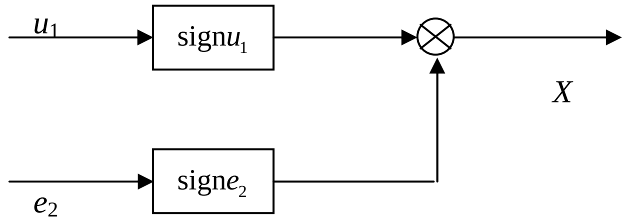

Fig. 10

The output signal after the multiplier is $X = a\left(\frac{\pi}{2} - \varphi\right)$, where a is a proportionality coefficient, and φ is the phase of e_2, reduced to the one of u_1. An apriori rotation of e_3 at $\frac{\pi}{2}$ is more convenient, so that the output signal becomes linearly dependent on the phase difference in amplitude and in sign.

Approximation of the criterion for symmetry is possible. One possible approximation is the equalization in module of two of the voltages. Such an approach, without being perfect, is too close to the optimal one, its hardware implementation being simple and reliable. The principal diagram is shown on Fig. 11.

The output signal is proportional to the difference between the voltages u_1 and u_2. Depending on the polarity of *X*, a control action is realized in one of the two directions, when the upper or lower thresholds are affected. Since the difference signal is obtained from one semi-wave of the voltages u_1 and u_2 only, the pulsations can be considerable. In order not to prolong unduly the averaging interval, it is suitable to account the difference signal after a whole number of semiperiods. With such reading the difference signal can be seen for every period of the network. This is naturally simplified by the circumstance that due to the phase difference between u_1 and u_2, there exists an interval of $\frac{2}{3}\pi$, during which X remains unaltered. A big pulsation of X is feasible at such synchronous accounting of the difference signal. The pulsation of X is determined not by the time constant R_0C, which is always multiple bigger than the period of the network frequency, but by the value of the capacitor C.

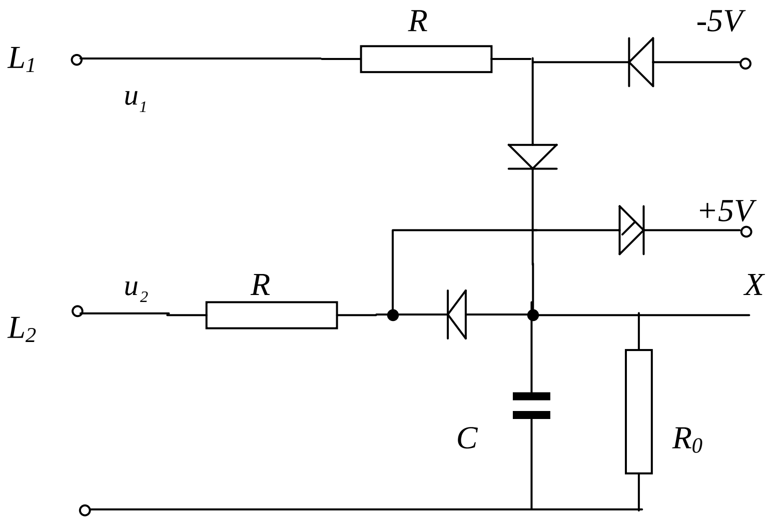

Fig. 11

The pulsation of the difference signal at equality of the voltages compared is determined by the changes of the charge on C. With respect to the phase difference $\frac{2}{3}\pi$ between the compared voltages u_1 and u_2, the charge alteration is defined by the expression

$$\Delta Q = \frac{U\sqrt{2}}{R\varpi}.\left[\int_0^{\frac{2}{3}\pi} \sin\theta d\theta - \int_0^{\frac{\pi}{3}} \sin\theta d\theta\right] = \frac{\sqrt{2}U}{R\varpi}$$

which leads to voltage pulsation

$$\Delta e = \frac{U\sqrt{2}}{CR\varpi}\ .$$

For the problem discussed, $u = 380$ V, $R = 470$ kΩ, $\varpi = 314$, $C = 4.7$ μF and $\Delta e = 770$ mV.

At difference of the voltages compared $\Delta u = u_1 - u_2$, the averaged value of the difference voltage e is defined by the condition for equality of the difference charge and discharge through resistor R_0 for a complete network period

$$\frac{e}{R_0}T = \frac{\Delta U 2\sqrt{2}}{R\varpi}, \quad e = \frac{R_0}{R}\frac{\sqrt{2}}{\pi}\Delta U.$$

Presenting the difference Δu in %, the expression becomes

$$e = \frac{e_0}{R}.\frac{\sqrt{2}}{100\pi}U_N\varepsilon.$$

Here U_N is the nominal effective value of u_1, and $\varepsilon = \frac{\Delta u}{U_N}100$

For the case considered $R_0 = 20$ kΩ, $R = 470$ kΩ, $U_N = 380$ V,

$$e = 72.8\varepsilon \text{ mV},$$

$$e_0 = 72.8 \text{ mV per 1\%}.$$

Such sensibility is too high and does not set any special requirements on the conventional threshold detectors of norm and deviation in a direct or inverse direction.

Another possible criterion of control is with respect to currents equalization in module, related to the load in the two phases, towards which the symmetrizing capacitors are connected. Such an approach is particularly appropriate for loads that are sensitive to current symmetry, such as deep pumps with long and hollow axes.

The control signal can be generated by current transformers after rectification and differential connection, as shown on Fig. 12.

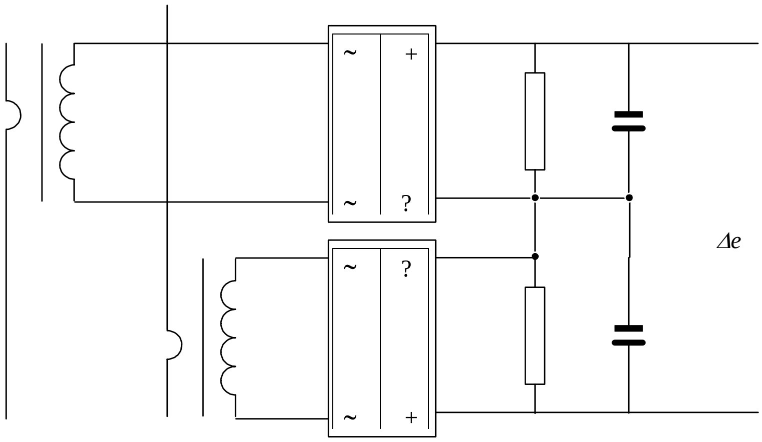

Fig. 12

Unlike voltages, the current is altered in wide limits and the signal formed will be linearly dependent on the absolute, not on the relative difference between the currents.

4. Conclusion

Triphase energy is the basic one in obtaining rotational mechanics, thanks to the particular ease of creating oriented rotating magnetic field. This energy is supplied to the main type of motors in manufacturing – asynchronous motor with a cage rotor. However, this energy is not available everywhere. This concerns mainly some rural and desert districts, where providing triphase energy is too expensive. This refers also to the cases, when the households are supplied with single phase or bi-phase energy and the application of different techniques requires triphase energy supply.

The work above presented discusses dynamic converters of monophase into triphase voltage, using a standard triphase asynchronous motor with a cage rotor as a main component. According to the concept presented, the converter shows the following advantages:

- it is functionally simple;
- built up from highly reliable components, that have proved their fitness in very long exploitation;
- a motor with century-old qualities is used;
- it enables the connection of several consumers, including monophase ones;
- with the help of some not complex means the start moment can be raised, that allows the switching on under nominal load or rapid acquiring of nominal revolutions;
- its price is not high in comparison with devices, converting monophase into tri-phase energy with different degree of symmetry, which is still quite expensive, not sufficiently reliable and requires qualified exploitation..

We believe that the converters presented will find wide application in the near future.

References

1. De Oliveira, S. Operation of Three-Phase Induction Motors Connected to One-Phase Supply. – IEEE Trans. Energy Conversion, Vol. **5**, December 1990, No 4, 713-718.
2. Badr, M. A., A. I. Aloloh, M. A. Abdel-Halim. A Capacitor Start Three Phase Induction Motor. – IEEE Trans. Energy Conversion, Vol. **10**, December 1995, No 4, 675-680.
3. Boglietti, A., A. Cavagnino, L. Ferraris, M. Lazzari. Induction Motor Equivalent Circuit Including the Stray Load Losses in the Machine Power Balance. – IEEE Trans. Energy Conversion, 2008, No 4.
4. Al-Bahrani, A. H., N. H. Malik. Steady State Analysis and Performance Characteristics of a Three-Phase Induction Generator Self Exited with a Single Capacitor. – IEEE Trans. Energy Conversion, Vol. **5**, December 1990, No 4, 725-732.
5. Mahato, S. N., S. P. Singh, M. D. Sharma. Capacitors Required for Maximum Power of a Self-Exited Single-Phase Induction Generator Using a Three-Phase Machine. – IEEE Trans. Energy Conversion, Vol. **23**, June 2008, No 2, 372-381.

6. C h a n, T. F., L o i L e i L a i. Capacitance Requirements of a Three-Phase Induction Generator Self-Exited with a Single Capacitance and Supplying a Single-Phase Load. – IEEE Trans. Energy Conversion, Vol. **17**, March 2002, No 1, 90-94.

Динамический конвертор монофазного напряжения в трифазное напряжение. Часть II: Старт и управление

Здравко Николов, Чавдар Корсемов, Христо Тошев

Институт информационных технологий, 1113 София

(Р е з ю м е)

Настоящая работа, представленна в двух частях этого издания, исследует подробно динамические фазовые конверторы, что помагает получить необходимые знания и завысимости для построения таких изделий. В первой части обсуждаются структура и компоненты конвертора. Во второй части исследуются старт и управление, которое приводит к заданной степени симметрии.